



Contents lists available at ScienceDirect

Journal of the European Ceramic Society

journal homepage: www.elsevier.com/locate/jeurceramsoc

Original Article

Chemical interpretation, enhanced ferroelectric property and dielectric breakdown strength of CuO-added $\text{Sr}_2\text{Nb}_2\text{O}_7$ ceramicsTao Chen^{a,b,c}, Ruihong Liang^a, Zhiyong Zhou^{a,*}, Kai Jiang^d, Zhigao Hu^d, Xianlin Dong^{a,*}^a Shanghai Institute of Ceramics, Key Laboratory of Inorganic Functional Materials and Devices, Chinese Academy of Sciences, 1295 Dingxi Road, Shanghai 200050, People's Republic of China^b University of Chinese Academy of Sciences, Shijingshan District, Beijing 100049, People's Republic of China^c ShanghaiTech University, 100 Haik Road, Shanghai 201210, People's Republic of China^d Key Laboratory of Polar Materials and Devices, Ministry of Education, Department of Electronic Engineering, East China Normal University, Shanghai 200241, People's Republic of China

ARTICLE INFO

Keywords:

Perovskite layered structure
Piezoelectricity
Ferroelectricity
Dielectric breakdown
Oxygen octahedron

ABSTRACT

The structural interpretation and electrical properties of perovskite layer structured (PLS) $\text{Sr}_2\text{Nb}_2\text{O}_7$ -xwt%CuO ceramics prepared by solid-state reaction method are investigated. The chemical interpretation of enhanced piezoelectricity is confirmed to be attributed to the rotation and/or distortion of oxygen octahedron caused by possible Cu^{2+} substitution at the A-site of $\text{Sr}_2\text{Nb}_2\text{O}_7$ by XRD refinement and variable-temperature Raman spectra. $\text{Sr}_2\text{Nb}_2\text{O}_7$ -xwt%CuO ($x = 0.3, 0.5$ and 0.7) ceramics shows enhanced ferroelectric properties with a larger P_r of $\sim 4.1 \mu\text{C}/\text{cm}^2$ and a smaller E_c of $\sim 63.1 \text{ kV}/\text{cm}$. This study further explains the cations in A-site play a major structural role in the polarization process for PLS system. It was found that dielectric breakdown strength increases up to $258.8 \text{ kV}/\text{cm}$ and then decreases gradually with the increase of CuO content. Impedance spectroscopy indicated that CuO addition could be helpful in increasing the grain boundary resistance then dielectric breakdown strength.

1. Introduction

Perovskite layer structured (PLS) piezoelectric ceramics are potential candidate materials in piezoelectric vibration sensors at high temperature for structural health monitoring, especially in the fields of the aerospace, nuclear plants, and automotive industries, due to their extremely high Curie points ($> 1300^\circ\text{C}$), excellent resistance to thermal depoling (almost up to $0.9T_c$) and high resistivity in high temperature (2–3 orders of magnitude higher than that of perovskite and BLSFs) [1–6]. However, it is difficult to achieve high piezoelectric constant because of relatively low bulk density and very few spontaneous polarization directions [7,8]. In general, the combinations of element doping and textured techniques were used to improve piezoelectric properties of PLS ceramics [4,9–11]. For example, Gao et al. prepared textured $\text{Sr}_{2-x}\text{Ba}_x\text{Nb}_2\text{O}_7$ ceramics by spark plasma sintering (SPS) which had an improvement of piezoelectric constant d_{33} up to $3.6 \text{ pC}/\text{N}^4$. Although many works have been carried out in PLS ceramics by this combination method, a breakthrough of piezoelectric constant d_{33} has not been achieved yet.

$\text{Sr}_2\text{Nb}_2\text{O}_7$ (SNO) is one of the most typical and promising PLS compound with an ultra-high T_c of 1342°C [12,13]. The crystal

structure of SNO is characterized by stacked perovskite layers containing corner-shared NbO_6 octahedron and 12-coordinated Sr cations. The perovskite layers are separated by rocksalt layers and the stacking is along the (010), which creates two nonequivalent A-sites that Sr1 atoms are existing in the perovskite layers and Sr2 atoms are located closer to boundaries [14,15]. López-Pérez showed $\text{La}_2\text{Ti}_2\text{O}_7$ (a member of PLS) is octahedral rotation-driven ferroelectricity and the spontaneous polarization from off-centering of Ti atoms (B-site) can be negligible by first principle approach [16]. On the other hand, Ning et al. designed an experiment to explore the effect of CeO_2 and WO_3 substitution at A and B sites in SNO ceramics, respectively [17]. They found that the piezoelectric property of A-site substitution is more obvious than that of B-site substitution. However, there is no definitive conclusion that the cations in A-site play a major structural role in the polarization process for PLS system.

Recently, we have reported that the introduction of 0.5 wt%CuO addition has significant effects on the sinterability, microstructure, and electrical properties of SNO ceramics prepared by solid state reaction method. SNO-0.5 wt%CuO ceramics show a remarkable d_{33} of $1.1 \text{ pC}/\text{N}$ while still with a very high T_c of 1340°C [18]. We supposed that the improvement of piezoelectricity could be attributed to the rotation of

* Corresponding authors.

E-mail addresses: zyzhou@mail.sic.ac.cn (Z. Zhou), xldong@mail.sic.ac.cn (X. Dong).<https://doi.org/10.1016/j.jeurceramsoc.2018.03.029>Received 21 November 2017; Received in revised form 13 March 2018; Accepted 18 March 2018
0955-2219/ © 2018 Elsevier Ltd. All rights reserved.

oxygen octahedron caused by possible Cu^{2+} substitution at the A-site of SNO, but it hadn't been confirmed yet.

Therefore, in this study, we further investigate underlying chemical mechanisms of the improvement of piezoelectric constant d_{33} and the structural evolution of SNO ceramics by CuO addition. It would be very helpful to understand the relationship between oxygen octahedral rotation and A/B-site substitution. In the meantime, the effects of the Cu^{2+} substitution on the ferroelectric property, thermal stability and dielectric breakdown strength of $\text{Sr}_2\text{Nb}_2\text{O}_7$ are reported.

2. Experimental procedure

Samples of $\text{Sr}_2\text{Nb}_2\text{O}_7$ -based ceramics with compositions of $\text{Sr}_2\text{Nb}_2\text{O}_7$ -xwt%CuO ($x = 0, 0.1, 0.3, 0.5$ and 0.7 , abbreviated as C0, C1, C3, C5 and C7) were prepared by solid reaction method. The details of preparation procedure were described elsewhere [18]. The crystal structure of ceramics was characterized by X-ray diffraction (XRD, D/MAX-2550V; Rigaku, Tokyo, Japan). The surface morphologies of the ceramics were observed using a scanning electron microscope (SEM, Hitachi, Tokyo, Japan). Raman spectra was carried out using a Jobin-Yvon LabRAW HR 800 UV (Paris, France) micro-Raman spectrometer (the exciting source was the 632.8 nm line from He-Ne laser). The ferroelectric hysteresis loops (P - E) were measured using a TF analyzer (Model 2000, aixACCT system, Aachen, Germany) at a frequency of 1 Hz at 150°C . A high-resistance meter (Model HP4339B; Hewlett-Packard) was used to measure the resistance at room temperature with applied voltages 400 V. The piezoelectric constants d_{33} were measured using a d_{33} meter (Model ZJ-3; Institute of Acoustics, Chinese Academy of Sciences, Shanghai, China). The accuracy of the d_{33} meter for measuring small coefficients was calibrated using X-cut quartz ($d_{33} = 2.3 \pm 0.1$ pC/N) [19]. Thermal depoling experiments were conducted by annealing the poled samples for 4 h at various high temperatures, cooling to room temperature, re-measuring d_{33} , and repeating the procedure at different temperatures up to 1300°C . The dielectric breakdown strength was measured by a voltage-withstand testing device (SD-DC 200 kV, China) with the samples immersed into silicone oil to prevent surface flashover. Complex impedance was measured by HP4294 LCR meter connected to a high-temperature horizontal tube furnace with continuous frequency scanning mode from 20 Hz to 10 MHz.

3. Results and discussion

Fig. 1(a) the XRD patterns of $\text{Sr}_2\text{Nb}_2\text{O}_7$ -xwt%CuO ceramics, which reveal the presence of no obvious secondary phases. The diffraction peaks of all ceramics can be indexed to the standard indexed peaks of $\text{Sr}_2\text{Nb}_2\text{O}_7$ orthorhombic structure (JCPDF No. 00-52-0321). Fig. 1(b)

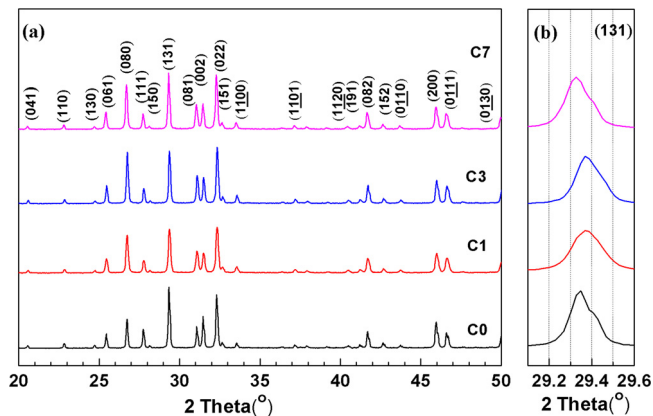


Fig. 1. XRD patterns of $\text{Sr}_2\text{Nb}_2\text{O}_7$ -xwt%CuO ceramics ($x = 0.0, 0.1, 0.3$ and 0.7) in the 2 θ range of (a) 20 – 50° , (b) 29 – 29.6° .

shows the zoomed highest peak (131) shifts gradually to higher angles as increasing x to 0.3 , which suggests crystalline interplanar spacing decreases. Further increasing x up to 0.7 results in the lower angles shift. This may be attributed to Cu^{2+} with smaller ionic size initially enter the A-site then the B-site due to the higher levels of CuO addition. Owing to the limitation of the resolution of the instrument, we cannot draw an accurate conclusion that Cu^{2+} was incorporated into the PLS crystal lattice.

Fig. 2 shows SEM morphologies of the surfaces of $\text{Sr}_2\text{Nb}_2\text{O}_7$ -xwt%CuO ($x = 0, 0.1, 0.3$ and 0.7) ceramics. It can be seen that the relative density of the ceramic samples increases and pores decrease with the increasing CuO content. Specifically, when x increases to 0.7 , some molten secondary phases can be observed at the surfaces. However, no any similar trace is observed from the fractural surface of C7 ceramics in the inset of Fig. 2(d). We classified these second phases which cannot be detected by XRD stem from excessive CuO. It could be assumed that excessive copper that concentrate at the grain boundaries tend to speed up mass transfer and migrate to surface during sintering process [20].

To further confirm whether Cu^{2+} enters the crystal lattice, XRD Rietveld refinements for the C0 and C5 ceramic powders were carried out to refine the lattice parameters, by using the GSAS-EXPGUI program [21,22]. The coordinates of $\text{Sr}_2\text{Nb}_2\text{O}_7$ with orthorhombic space group Cmc_2 were used as an initial structure model [15]. The refined profiles fitting well with the experimental data for C0 and C5 are shown in Fig. 3(a) and (b), respectively. The structure refinement conditions and crystal data of these two compositions are listed in Table 1. The reliability factors, R_{wp} , R_p and reduced χ^2 values are 9.43%, 7.39% and 4.821 for C0 and 10.69%, 7.68% and 7.537 for C5, respectively. The refined lattice parameters (a , b , c) are 3.9505 \AA , 26.6140 \AA , 5.7482 \AA for C0 and 3.9462 \AA , 29.0125 \AA , 5.2332 \AA for C5, respectively. The unit cell volume of C5 (599.164 \AA^3) is smaller than that of C0 (604.367 \AA^3). According to ionic radius and coordination numbers of Sr^{2+} (1.44 \AA , CN = 12), Nb^{5+} (0.64 \AA , CN = 6) and Cu^{2+} (0.73 \AA , CN = 6) [23], the unit cell volume would increase if Cu^{2+} replace Nb^{5+} at B-site. Therefore, Cu^{2+} is preferable to occupy larger Sr^{2+} at the A-site, which would tend to induce and enhance the distortion of oxygen octahedra. On the basis of the refined results, the crystal structures of C0 and C5 viewed along c -axis are depicted with the VESTA program [24] in the insets of Fig. 3(a) and (b), respectively. It can be seen that Cu^{2+} ions substitution for Sr^{2+} at A-site are existing in the perovskite layers rather than boundaries, which is in good agreement with the refined unit parameters that a and c decrease while b increases.

In order to understand the relationship between oxygen octahedra rotation and A-site substitution in the PLS system, Raman spectra of $\text{Sr}_2\text{Nb}_2\text{O}_7$ -xwt%CuO ceramics are shown in Figs. 4 and 5. Generally, Raman modes are sensitive to the rotation or distortion of oxygen octahedra for layered perovskite-like materials and Raman spectra at elevated temperature can provide clear evidence to explain oxygen octahedral evolution [10,25,26]. Fig. 4 shows the temperature dependence of Raman spectra for the C0 ceramic measured from 30°C to 500°C . Theoretically, the modes below 200 cm^{-1} are related to the vibration of A-site ions and the modes above 800 cm^{-1} stem from the stretching of B–O bonds. The peaks at 101 , 142 , 175 and 845 cm^{-1} have a red shift of frequency with increasing temperature, which can be due to the thermal expansion of the lattice according to the perturbation model [27]. Notably, the modes at 572 cm^{-1} exhibit a remarkable low-frequency shift and the peak become weaker with increasing temperature, which are likely to be associated with the rotation or distortion of NbO_6 octahedron. For oxygen octahedral rotation-driven ferroelectricity, the weakening and the disappearing of modes at higher temperature are assigned to the rotation or distortion of oxygen octahedron and the improvement of structural symmetry [25,28]. Fig. 5 shows the Raman spectra of $\text{Sr}_2\text{Nb}_2\text{O}_7$ -xwt%CuO ceramics from 80 to 1000 cm^{-1} at room temperature. It is observed that the mode at 572 cm^{-1} gradually tends to high frequency shifting and does not become weaker in the regionally enlarged drawing. Comparison with the

Download English Version:

<https://daneshyari.com/en/article/7898159>

Download Persian Version:

<https://daneshyari.com/article/7898159>

[Daneshyari.com](https://daneshyari.com)